Macroscopic Solvent Polarization-Induced Reorganization of the Electron Density in Different Excited States: A Study on Formaldehyde Molecule by a Multiconfiguration Self-Consistent Reaction-Field Method

CHITRANI MEDHI,[1] S. P. BHATTACHARYYA[2]

[1]*Department of Chemistry, Guwahati University, Guwahati 781014, India*
[2]*Department of Physical Chemistry, Indian Association for Cultivation of Science, Jadavpur, Calcutta 700032, India*

ABSTRACT: A detailed study of the type and extent of electronic reorganization created by macroscopic solvation of a prototypical carbonyl solute is carried out within the framework of the semiempirical multiconfiguration self-consistent reaction-field model. The solvation causes additional polarization of the electronic charge density within the carbonyl group. Orbitalwise breakup of the electron densities on the key atoms throws light on such features as the polarity dependence of inversion barriers and out-of-plane bending. Macroscopic solvation is shown to cause a reverse π-polarization within the carbonyl group, affecting barrier heights on the inversion path. © 1998 John Wiley & Sons, Inc. Int J Quant Chem 70: 415–428, 1998

Introduction

It is the common experience of a physical chemist, a biophysicist, or a chemist that the response of a "solute" to a given experimental probe is often modulated, sometimes profoundly, by the presence of a particular environment [1, 2]. Theoretical modeling of the environmental modulation of solute properties is receiving increasing attention nowadays. The study of the interaction between a solute and solvent is complicated and has been handled theoretically through models of varying degrees of sophistication. These models can be divided into three groups: (i) the discrete

model, (ii) the continuum model, and (iii) the quasicontinuum model.

In the discrete model, a finite number of solvent molecules are assumed to surround the solute molecules and all molecules, of the solutes or solvents, are treated explicitly. The model focuses on the description of short-range interactions and the results often depend critically on the number of solvent molecules used in modeling the surrounding of the solute species [3–8]. Models of this kind may be suitable for describing specific solvent effects such as hydrogen bonding, charge transfer between the solute and solvent, and exchange effects. It is mostly applied to systems where the solvent structure is well defined, for example, when the interaction between the solute and solvent is strong. The use of the discrete model may, however, become problematic when strong dynamic coupling between the structure and potential exists or when cooperative field effects from a large number of molecules affect the short-range interaction as is often found to happen in polar systems.

Calculations using discrete models have been done at ab initio or semiempirical SCF levels. Researchers have experimented with the use of point charges or dipoles for the solvent molecules and used the Monte Carlo or molecular dynamics methods for simulation.

In the continuum models, the solvent is described by a homogeneous continuous medium characterized by a macroscopic dielectric constant. The solute molecule is assumed to interact with the surrounding polarizable dielectric medium through a reaction field (RF). This RF arises from the charges induced in the medium surrounding the solute charge system. Two approaches are common: (a) the cavity model [9–14] and (b) the effective or image charge model [15, 16]. The continuum models allow one to take into account long-range interactions. However, they cannot describe the short-range interactions such as dielectric saturation effects in aqueous ionic solutions, that is, these models do not discriminate water molecules close to the dissolved ions which behave differently from the water molecules in the bulk. The continuum model has, therefore, been further generalized to two concentric dielectric continua [11–14] and, recently, even to anisotropic continua [14b]. The quasicontinuum models combine essential features of both the discrete and continuum models. They work by constructing a solvation shell containing a finite number of sol-

vent molecules which are treated explicitly. Outside this region, the solvent is modeled by a discrete continuum.

Continuum models have been quite popular among chemists in general. Klopman [15] suggested a simple physical model for incorporating solvent effects in theoretical calculations. In this model, one performs LCAO−MO−SCF calculations on an isolated solute molecule first (either at the ab initio or semiempirical level) and then uses the MO coefficients to compute the solute−solvent interaction energies through electrostatics. The weakness of this approach is that the solute MOs do not reflect the presence of the solvent. One can immediately think of incorporating the electrostatic interaction in the Hamiltonian characterizing the solute charge system in the presence of the solvent and somehow using this modified Hamiltonian to perform SCF(MO) calculation of the solute wave function, which would then reflect the effects of solute−solvent interactions approximately. Germer [16] developed a simple model of this kind assuming that the polar nature of the solvent can be characterized by a single macroscopic solvent parameter, the dielectric constant (ε), and developed a semiempirical MO method incorporating solute−solvent interactions through a simple electrostatic model. The theoretical model proposed by Germer assumes that the presence of the solute charge system in the polarizable medium creates a number of charges in the surrounding solvent, which interact further with the solute charges, the strength of the interaction depending on the polar nature of the solvent. The assumed form of the solute−solvent interaction energy was simply the Born energy for ionic solvation.

Although arguments can be given for its use, the model lacks rigorous theoretical justifications. Tapia and Goscinski [17] developed a formal quantum mechanical reaction-field theory of the solvent effects which reduced to the Onsager model as a limiting case. Their variational formulation for the ground state led to an effective nonlinear Hamiltonian for the solute molecules in solution. The theory has been implemented numerically for the solvation of a molecule in the ground state at the CNDO/2 level and the result obtained indicates the feasibility of implementing the self-consistent reaction-field (SCRF) scheme. Constanciel and Tapia [18] gave a simple electrostatic analysis of the virtual charge (solvation) model of representing the environmental effects on the electronic wave function of the solute immersed in the polar-

izable surrounding. These authors could derive a modified Hartree−Fock type of operator (h_{eff}) correctly. The eigenfunctions of h_{eff} represented an electron in a molecular orbital subjected to the average field of the other electrons and to the RF produced by the virtual charges created in the medium by the solute charge system. A correct choice of the functional to be minimized is necessary to ensure self-consistency of the solute−solvent interaction and account for solvent reorganization or polarization effects systematically. RF effects on the electron distribution and chemical reactivity of the molecules was also studied by Karelson et al. [19] using the cavity model. On the basis of ab initio, INDO−SCF, and INDO/CI calculations, these authors concluded that the introduction of a dielectric medium seems to have little effect on the calculated geometry, although it allows local charges to develop in the system. As to the effect of the RF on a chemical reaction, these authors noted that the HF molecule dissociates heterolytically in a solvent of a dielectric constant of 80 even when electron correlation is included.

A search of the literature tends to suggest that the continuum models have been explored generally in the context of closed-shell SCF theory. A more generalized version of the SCRF theory that would allow one to carry out studies on more general systems and states which may not be amenable to treatment by closed-shell HF theory has been recently proposed [20, 21] and applied to a number of interesting problems [22−26]. These multiconfiguration SCRF methods have opened up the possibility of studying media effects on spectroscopic and kinetic properties of molecules.

Our interest lies in the electronic structure of a solute molecule modulated by a solvent which is present in a large excess (1 solute molecule + N solvent molecules in a volume V at a temperature T K). We know that in a polar solute charge separation may occur and any such process would inevitably bring in large coupling with the surrounding media. What is going to be the effect of this coupling on the solute electronic structure or for that matter on the solute properties? One immediately understands that the answer to this question lies in a proper quantum mechanism description of the solute subsystem coupled to the N-solvent molecules via electrostatic interactions (neglecting small relativistic and retardation effects). This would require us to solve, subject to approximate boundary conditions, the many-particle Schrödinger equation describing the motion of all the nuclei and electrons coupled together:

$$\hat{H}\Psi = \left[\sum_i - \frac{\hbar^2}{2m_i} P_i^2 + \sum_{i<j}\sum \frac{q_i q_j}{r_{ij}} \right]\Psi$$
$$= \frac{-h}{i}\left(\frac{\delta\Psi}{\delta t} \right). \tag{1}$$

The idea is, however, too complicated to afford detailed calculations. This has led to the search for an effective Hamiltonian which depends only on the solute coordinates. Different approaches are available in the literature for constructing the effective solute Hamiltonian. Without going into details of the derivation, we may sum up by noting that these methods generally end up with constructing an effective nonlinear Schrödinger equation [23]:

$$\{H_0 + V[\phi\phi^+]\}\phi = \lambda\phi, \tag{2}$$

where H_0 is the free solute Hamiltonian and $V[\phi^+\phi]$ represents the effective solute solvent interaction term. The $[\phi^+\phi]$ term in square brackets denotes the dependence of the potential V on the solute electron density, thereby making Eq. (2) effectively a nonlinear Schrödinger equation [17, 27]. There are various approximate schemes for the construction of the effective potential V. The RF approach in a variationally correct formulation can often be an effective way of handling the problem. In what follows, we consider such a possibility.

Method

Our purpose in this section will be to construct a suitable multiconfiguration self-consistent reaction-field (MC−SCRF) theory which can handle the solvation of a molecule in the ground and excited states with equal facility. Unlike the authors of [20], we do not adopt the Onsager RF model. Rather, we chose the image charge representation of the field [21].

By solvation, we mean only nonspecific or macroscopic effects arising from the solvent polarization induced by the solute charge system. Our main interest will be in the excited states of molecules where a substantial electron-density reorganization occurs as a result of excitation. In the context of electronic structure theory, specific (microscopic) solvation, as we have already noted, is traditionally treated by the supermolecular ap-

proach. It considers the solute–solvent pair as a single quantum mechanical system. Any nonspecific solvation effects arising between the solute molecule and the electric field arising from the polarization of the solvent is usually handled by applying some statistical mechanical approach, for example, the Monte Carlo or molecular dynamics methods. The execution of the step, however, requires an appropriate intermolecular potential surface which is usually taken as the Born–Oppenheimer surface of the free solute molecule interacting with an isolated solvent molecule. This approach may be adequate unless macroscopic solvation profoundly affects the electron-density distribution within the solute molecule, thereby affecting the intermolecular potential energy surface on which the simulation is done. It is therefore important to have a clear understanding of the type and extent of electronic reorganization that the macroscopic solvation can bring about.

Let $\tilde{\Psi}$ be the trial wave function for an n-electron system in a given electronic state. We assume that $\tilde{\Psi}$ has been expanded in terms of a set of configuration functions $[\phi_I]_{I=1}^M$:

$$\tilde{\Psi} = \sum_{I=1} C_I \phi_I. \tag{3}$$

In Eq. (3), ϕ_I's are Slater determinants constructed from a set of N orthonormal molecular spin orbitals $[\phi_i]_{i=1, n}$:

$$\phi_I = \frac{1}{\sqrt{N!}} \left| \phi_1 \ \overline{\phi}_2 \ \cdots \ \phi_{n-1} \ \overline{\phi}_n \right|. \tag{4}$$

Each MO is again written as a linear combination of a fixed set of r ($r > n$) atomic basis functions (χ):

$$\phi_I = \sum_{p=1}^r T_{pi} \chi_p. \tag{5}$$

Written in matrix notation, we have the following linear transformation between n occupied MOs and the r atomic orbitals [Eq. (6)]:

$$\phi(\phi_1 \ \cdots \ \phi_i \ \cdots \ \phi_n) = (\chi_1 \ \cdots \ \chi_i \ \cdots \ \chi_r)T. \tag{6}$$

The energy of the system is given by

$$E = \langle \tilde{\psi}|H_0|\tilde{\psi}\rangle = TrhTP_1 + \frac{1}{2}TrZ(P_2)T^\dagger. \tag{7}$$

P_1 and P_2 are the one- and two-electron density matrices in the $\{\phi\}$ basis. If we now assume that

the solute molecules are in contact with a polarizable medium (the solvent), the Hamiltonian will have a solute–solvent interaction term and an appropriate functional would have to be constructed.

Let us consider a modified functional $\tilde{\varepsilon}$ which contains a solute–solvent interaction component through a suitable RF model:

$$\tilde{\varepsilon} = \langle \tilde{\Psi}|H|\tilde{\Psi}\rangle - \beta\langle \tilde{\Psi}|\tilde{\Psi}\rangle + \frac{1}{2}\langle \tilde{\Psi}|H(\tilde{\Psi})|\tilde{\Psi}\rangle. \tag{8}$$

β is the Lagrangian multiplier connected with the normalization constraint. The RF potential $\tilde{\nu}(R)$ acting on the solute molecule is defined through an image charge-density operator (ρ_v) acting on the charge particles of the system [18]:

$$\tilde{\nu}(R) = \int \frac{dR' \langle \tilde{\Psi}| \hat{\rho}_v(R')|\tilde{\Psi}\rangle}{|R - R'|}. \tag{9}$$

$\rho_v(R')$ is a simple n-electron image charge-density operator represented as follows:

$$\rho_v(R') = f(D)\left[\sum_A Z_A \delta(R' - R) - \sum_{I=1} (R' - r_i) \right]. \tag{10}$$

The first summation runs over different atoms (A) in the solute molecule, the atom A being characterized by the nuclear charge Z_A. The second summation runs over the number n of the solute electrons. $\delta(R' - R)$ is Dirac's delta function. With this definition of $\rho_v(R')$, we can now write

$$\langle \tilde{\Psi}| \hat{\rho}_v(R')|\tilde{\Psi}\rangle$$
$$= f(D) \sum_A Z_A \delta(R' - R) - \langle \tilde{\Psi}|\sum_i \delta(R' - r_i)|\tilde{\Psi}\rangle$$
$$= f(D)\left[\sum_A Z_A \delta(R' - R) - \sum_{ij} P_{ij}\phi_i^+(R')\phi_j(R') \right]. \tag{11}$$

$[P_{ij}]$ are the elements of the one-electron density matrix in the MSO basis. If one uses natural orbital representation, one can rewrite Eq. (11) as follows:

$$\langle \tilde{\Psi}| \hat{\rho}_v(R')|\tilde{\Psi}\rangle$$
$$= f(D)\left[\sum_A \delta(R' - R_A) - \sum_{n_i} n_i \phi_i^+(R')\phi_i(R') \right] \tag{12}$$

(the n_i's are the natural orbital occupation numbers).

The solute–solvent interaction term appearing in the solvent-modified solute energy functional ε can therefore be written in the image charge representation of the RF as follows:

$$H' = V(R) = f(D)\left[\sum_A V_A(R) - \sum_i V(r_i)\right]. \quad (13)$$

The term $f(D)$ is dependent on the microscopic solvent dielectric constant in the following way [18]:

$$f(D) = -(1 - D^{-1}) = -\left(1 - \frac{1}{\sqrt{\varepsilon}}\right). \quad (14)$$

D may therefore be thought as an effective dielectric constant of the solvent. Once H is defined, our next task is to make ε stationary with respect to (i) variations in the linear expansion coefficients $[C_I]$ and (ii) variations in the orbital forms $[\phi_I]$. Following the standard procedure of the first-order variation, we arrive at two sets of equations, namely, a CI-like equation and a modified MC–SCF orbital equation which should be solved in tandem:

$$\tilde{H}\tilde{C} = \tilde{E}\tilde{C} \quad (15a)$$

$$\tilde{V} = S\tilde{T}\beta, \quad (15b)$$

where

$$\tilde{V} = \tilde{h}\tilde{T}P_1 + \tilde{Z}. \quad (15c)$$

$\tilde{h}$ in Eq. (15c) represents the one-electron part of the MC–SCF operator which includes the effects of solvent polarization in the image charge representation of the solvent RF. P_1 stands for the one-electron density matrix in the ϕ basis (ϕ's are the solvent-modulated solute orbitals). The solvent-modified two-electron part of the MC–SCF operator is given by $\tilde{Z}$, a typical matrix element of which reads

$$\tilde{Z}_{PI} = \sum_{jkl}^{MO} \sum_{qrs}^{AO} \tilde{T}\langle pq|rs\rangle \tilde{T}_{rk}\tilde{T}_{sl}\tilde{P}_{2kl,ij}. \quad (16)$$

$\tilde{P}_2$ in Eq. (16) represents the two-electron density matrix in the ϕ basis. Equation (15a) is a typical matrix eigenvalue equation and can be solved easily. Equation (15b) is not amenable to such straightforward solution. One can invoke the method of steepest descent or conjugate gradient to solve for T [28]. But they converge rather slowly.

So, we have adopted the orthogonal gradient method [29, 30] for solving Eq. (15b). It is perfectly feasible, in principle, to apply this model in an ab initio framework. However, that will be computationally costly.

To evaluate the performance of the model and to have some idea about the type and extent of the solute electron-density distribution, we applied the theory at the INDO level of approximation. Standard INDO approximations have been used throughout except for the evaluation of two-center matrix elements of h which are estimated by applying Mullikens' approximation, that is,

$$\begin{aligned}
\tilde{h}_{pq}^{AB} &= \langle \chi_p^A|\tilde{h}|\chi_q^B\rangle \\
&= \langle \chi_p^A|h^0|\chi_q^B\rangle + \langle \chi_p^A|h'|\chi_q^B\rangle \\
&= \left(h_{pq}^0\right)_{INDO}^{AB} \\
&\quad + 1/2\left[\langle \chi_p^A|h'|\chi_p^A\rangle + \langle \chi_p^B|h'|\chi_q^B\rangle\right]S_{pq}^{AB}.
\end{aligned} \quad (17)$$

h^0 has the standard form of the one-electron part of the INDO Hamiltonian and h' is the solvent modification of it. h_{pq}^0 is evaluated by the standard INDO approximations. Mulliken's approximation is therefore used only for the additional terms arising from the solvent contribution to h. Although the SCRF models like the one described here can be quite useful, it is important to point out the limitations of the approach. These limitations stem partly from the slowness of the relaxation of solvent orientational polarization (P_{or}) as it involves nuclear motion. The immediate consequence is that P_{or} does not follow the Franck–Condon (FC) electronic transitions and, hence, excited states are not under equilibrium solvation immediately after their creation. The equilibrium SCRF theories cannot therefore address the problems of FC excited states.

The excited states at equilibrium, on the other hand, bring in a different kind of difficulty that has its origin in the nonlinear nature of the SCRF. This nonlinearity manifests itself in generating different effective solvent-modulated Hamiltonians for different excited states which are therefore nonorthogonal (unless they have different spatial or spin symmetries) and are not physical states. A way to bypass the problem could be to adopt a state-averaged RF model which optimizes the equilibrium reaction field for a number of states on the average. In our cases, all the states are orthogonal either because of spatial symmetry or

because of spin symmetry. These problems are generally overlooked in dealing with SCRF theories. The issues involved have been elaborately discussed by Hynes and Kim in a number of publications [31–36].

The third point that requires careful examination concerns the cavity size (in Onsager's RF model) or the g-factor (in Tapia's RF model) to be used in the SCRF model. The model described here uses image charge representation of the RF and, hence, Tapia's g-factors are the equivalents of the cavity sizes that are used to be determined. This is important in view of the recent demonstration by Berne that the cavity size may be considerably different for different electronic states [25]. In our calculations reported in the sections that follow, we used identical g-factors for both the ground and excited states by setting the parameter g'_{AB} representing the interaction energy of the image charge created by atom A with the electrons on atom B equal to γg^0_{AB}, where γ is a scale factor and g^0_{AB} is the corresponding electron repulsion parameter used in the solute electronic Hamiltonian. We have used $\gamma = 1$ throughout for formaldehyde. However, the possibility of using different values of γ for different electronic states exists in our model.

Results and Discussion

We report in this section some interesting results obtained by the application of the model outlined in the preceding section. At the outset, let us make our objective clear: Our main purpose will be to examine the nature of the reorganization of the solute electron density that is brought in by macroscopic or nonspecific interaction and compare it with whatever reorganization is caused by a specific interaction. Our focus is on excited states which invoke fairly large intermolecular electronic redistribution, for this gives us an opportunity to study the interplay of the solvation-induced relaxation of charge densities with that caused by excitation. The system that we have chosen is a prototypical carbonyl system, for example, which has been the target of so many theoretical and experimental investigations. The trial wave function has been chosen in the simplest admissible form:

$$^{1,3}\Psi_{i-j} = 1/\sqrt{2}\Big[|\phi_1\ \overline{\phi}_1\ \cdots\ \phi_i\ \overline{\phi}_j\ \cdots\ \phi_n\ \overline{\phi}_n|$$
$$+ (-1)^s|\phi_1\ \overline{\phi}_1\ \cdots\ \phi_j\ \overline{\phi}_i\ \cdots\ \phi_n\ \overline{\phi}_n|\Big].$$

Geometry optimization was carried out wherever required by a pattern search method.

MACROSCOPIC SOLVATION-INDUCED STRUCTURAL REORGANIZATION IN SOLUTE

The type of electronic reorganization in the excited states of H_2CO caused by macroscopic solvation noted earlier [21] led us to speculate about the possible consequences of such reorganizations. One such possibility is structural changes brought about in the molecule by the solvent-induced relaxation of electron density. Table I summarizes the optimized geometrical parameters of the forced planar and fully relaxed (i.e., the condition of forced planarity of the solute molecule is relaxed) formaldehyde molecule in the $^3n\pi^*$ state in four different solvents, each being characterized by an appropriate macroscopic solvent dielectric constant. The computed data indicate that the equilibrium $C{=}O$ bond length increases considerably as the polarity of the solvent increases. The increase is fairly large initially and saturates at higher polarities to a value 1.34 Å. The $H{-}C{-}H$ angle is also seen to widen a bit as the solvent polarity increases. It is clearly revealed that the out-of-plane angle (ϕ) increases slowly with increase in the solvent polarity. A considerable stretching of the $C{=}O$ bond length is again noted. The removal of the constraint (of planarity) strongly affects the equilibrium $H{-}C{-}H$ angle which is now seen

TABLE I _____
Computed geometrical parameters of forced planar and fully relaxed H_2CO molecule in the $^3n\pi^*$ state in solvents of different degrees of polarities.

Molecule in	Solvent dielectric constant (ε)	Bond lengths (Å)		Angles (degrees)	
		C=O	C—H	HCH	ϕ
Forced planar	1	1.318	1.108	124.4	0.0
	20	1.329	1.110	128.5	0.0
	40	1.335	1.108	129.6	0.0
	60	1.338	1.109	130.3	0.0
	80	1.339	1.109	130.7	0.0
Fully relaxed	1	1.315	1.107	125.3	36.5
	20	1.333	1.109	121.5	36.6
	40	1.337	1.109	121.5	38.1
	60	1.340	1.109	122.0	39.0
	80	1.342	1.109	122.0	39.5

FIGURE 1. Inversion profile of forced planar H_2CO in solvents of dielectric (20–80) in $^3n\pi^*$ state.
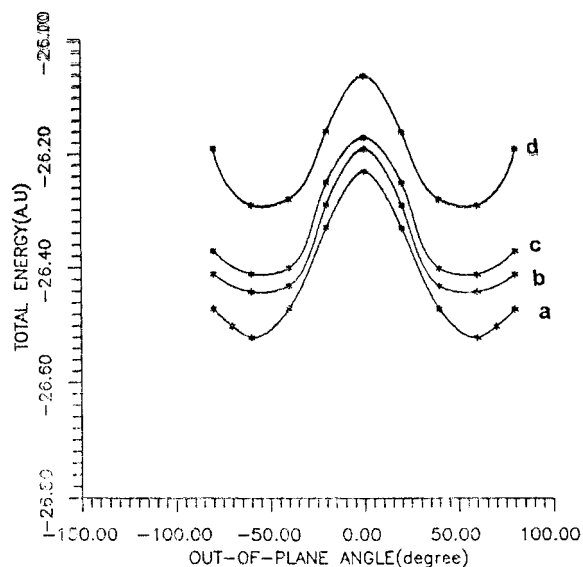

FIGURE 2. Inversion profile of fully relaxed H_2CO in solvents of dielectric (20–80) in $^3n\pi^*$ state.

to narrow down considerably from the corresponding solvent free value as the dielectric constant of the solvent (ε) increases from 1 to 20 and then remains more or less fixed at about 121–122° even when the polarity would immediately suggest that the planar inversion process at the carbonyl carbon center would be affected by macroscopic solvation.

Figures 1(a)–(d) display planar inversion profiles of H_2CO in the $^3n\pi^*$ state in solvents of different polarities ($\varepsilon = 20$–80). While constructing these inversion profiles, complete geometry optimization was carried out at each value of ϕ in all the solvents, that is, we have assumed that complete relaxation of the solute molecular and electronic structure occurs during the process of inversion. The corresponding inversion profiles for the cases where structural relaxation during the inversion is not allowed to occur are exhibited in Figure 2(a)–(d). The two sets of profiles do not qualitatively differ much. The profiles do indicate, however, that the barrier to inversion increases with solvent polarity. The dependence of the barrier on the polarity of the solvent revealed by the inversion profiles shows that even nonspecific (macroscopic) solvation can influence an intramolecular process like inversion very significantly. We will analyze the nature or polarity dependence of the inversion barrier and possible origin of it later. Before that, we examine the effects that macroscopic solvation could have on
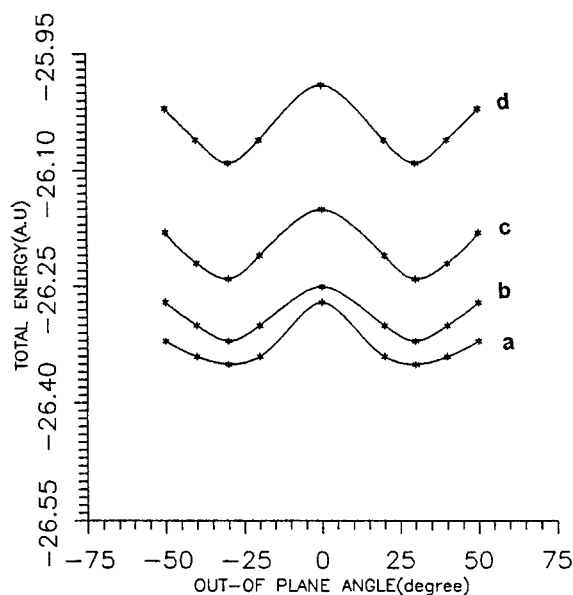
our prototypical system in the $^1n\pi^*$ or $^3\pi\pi^*$ states as well.

Table II displays the computed geometrical parameters (completely optimized) and the forced planar formaldehyde molecule in the $^1n\pi^*$ state in solvents of widely different values of the dielectric constant. Just as observed for in the $^3n\pi^*$ state, the $C=O$ bond length in the $^1n\pi^*$ state is predicted to increase substantially with increase of the sol-

TABLE II
Computed geometrical parameters of fully relaxed and forced planar H_2CO in the $^1n\pi^*$ state in solvents of different degrees of polarities.

Molecules in	Solvent dielectric constant (ε)	Bond lengths (Å)		Angles (degrees)	
		C=O	C—H	HCH	ϕ
Fully relaxed	1	1.320	1.107	122.4	28.3
	20	1.345	1.106	123.2	35.4
	40	1.349	1.107	124.2	36.8
	60	1.352	1.107	124.4	37.6
	80	1.353	1.107	124.6	37.3
Forced planar	1	1.320	1.105	124.0	0.0
	20	1.340	1.106	128.5	0.0
	40	1.347	1.106	130.7	0.0
	60	1.350	1.105	131.0	0.0
	80	1.351	1.105	131.0	0.0

vent polarity first and then saturate at a value of $r = 1.35$ Å at $\varepsilon = 60$. The noticeable effect of macroscopic solvation in the $^1n\pi^*$ state concerns the equilibrium out-of-plane angle which is also seen to increase with increase of the polarity. The patterns of increase in $r\,(C{=}O)$ and ϕ are almost the same. Here, also, one finds the planar inversion barrier to be dependent on the polarity of the solvent. Except for fairly large changes in the $H{-}C{-}H$ angle at the forced planar geometry, the other features follow the trend already noted in the optimized geometry. Table III reports the macroscopic solvation-induced changes in the geometrical parameters of the formaldehyde molecule in the $^3\pi\pi^*$ state. The $C{=}O$ bond length and out-of-plane bending angle are seen to increase with increase in the macroscopic solvent polarity. The angle $H{-}C{-}H$, however, does not register any regular pattern of dielectric dependence in the $^3\pi\pi^*$ state.

MACROSCOPIC SOLVATION-INDUCED REORGANIZATION OF ELECTRON DISTRIBUTION IN SOLUTE

We have already noted that nonspecific solvation of the formaldehyde molecule in the $n\pi^*$ or $\pi\pi^*$ states significantly affects the molecular geometry, especially the out-of-plane bending coordinate (ϕ). In all the three states studied, ϕ appears to increase with increase of the solvent polarity, which in our model is measured by the macroscopic dielectric constant (ε) of the solvent. It also follows from the inversion profiles that the barrier to inversion increases with the inversion in ε. We now propose to look into the nature of the polarity dependence of the computed barriers to inversion in a given electronic state and try to establish a connection between the polarity depen-

dence of the barrier and electronic reorganization that takes place at the inversion center due to the solvent polarization. Figure 3(a)–(c) displays plots of the computed values of ϕ (equilibrium) in the $^{1,3}n\pi^*$ and $^3\pi\pi^*$ states of H_2CO against the dielectric function $f(D)$ of the solvents. The plots are found to be linear in each case. Figure 4(a)–(c) displays the profiles of the computed barrier heights when plotted against $f(D)$. The linearity of the polarity dependence of the inversion barriers is interesting as a similar polarity dependence of the barriers has been observed in different contexts [37, 38].

The observed increase in the barrier heights, however, needs to be rationalized. We may note that the $n\pi^*$ transition in the formaldehyde molecule has the attributes of an intramolecular charge-transfer transition in which an electron in an orbital (n) predominantly localized on the carbonyl oxygen is promoted to an orbital (π^*) having a higher amplitude on the carbon atom. The direction of the charge transfer ($O \rightarrow C$) therefore opposes the normal ground-state polarization of the charge density within the carbonyl group ($C^{+\delta}{=}O^{-\delta}$) and tends to build up excess electron density on the carbon atom. The $C{=}O$ bond order is also reduced nearly to that of a single bond. It would therefore be natural to expect that excess electron density on the atom must redistribute itself suitably. The essential features of the reorganization following $^{1,3}n\pi^*$ excitation in the $XYC{=}O$ type of molecule was recently studied in the solvent-free situation by Das et al. [39]. We could therefore concentrate on the role played by the solvent in modulating further the normal electronic reorganization that accompanies excitation in carbonyl chromophores.

Figure 5(a) and (b) display variations in the computed net charges on the C and O atoms (q_C and q_O, respectively) in the fully relaxed $^3n\pi^*$ state in solvents of different degrees of polarities. The plots of $|q_C|$ and $|q_O|$ against $f(D)$ are seen to be linear again and show that macroscopic solvation polarizes the electron density within the $C{=}O$ moiety toward the oxygen atom and therefore helps in the dissipation of the excess electron density created on the carbon atom by the $n \rightarrow \pi^*$ excitation in the absence of the solvents. How does out-of-plane bending affect this solvent-assisted polarization of the $C{=}O$ bond? To monitor that, we plotted the computed values of q_C and q_O of the partially relaxed H_2CO against $f(D)$ [Fig. 6(a) and (b)]. The plots are linear here also. But from

TABLE III
Computed geometrical parameters of fully relaxed H_2CO in the $3\pi\pi^*$ state in solvents of different degrees of polarities.

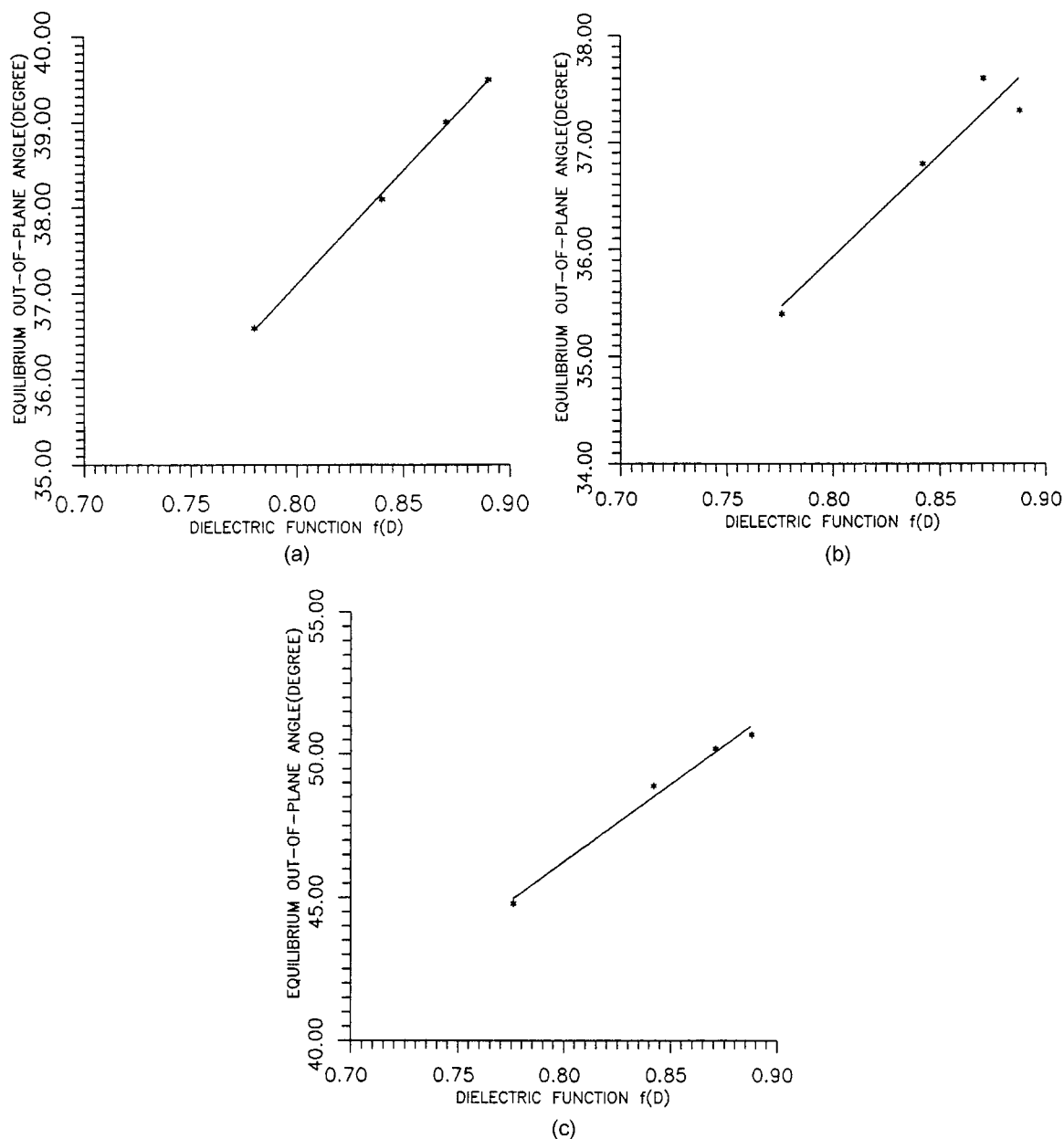| Solvent dielectric constant (ε)	Bond length (Å)		Angles (degrees)	
	C=O	C—H	HCH	ϕ
1	1.384	1.107	120.6	35.5
20	1.402	1.107	118.2	44.8
40	1.406	1.111	118.0	48.9
60	1.410	1.112	119.2	50.2
80	1.410	1.112	117.9	50.7

FIGURE 3. Inversion profile of H_2CO in solvents of dielectric (20–80) in the $^1n\pi^*$ state.

the values of q_C or $|q_O|$ at the forced planar and completely relaxed geometries (Table IV) for different values of ε, we can see that bending enhances the positive charge on the carbon atom and the net negative charge on the oxygen atom. Therefore, out-of-plane bending also provides an avenue for restoring the normal polarization of the π-electron density on the $C=O$ bond ($C^+=O^-$) and opposes the reverse polarization that accompanies the $n \rightarrow \pi^*$ excitation. The computed bar-rier heights in the fully relaxed inversion process have already been found to be a linear function of the dielectric function $f(D)$ of the solvents. The barrier heights for unrelaxed inversion in the $^3n\pi^*$ state are also found to be linear function of $f(D)$ (Fig. 7). The breakup of this net electron population on the carbon atom in the $n\pi^*$ states of fully relaxed and forced planar H_2CO in solvents of different polarity are recorded in Tables V and VI, respectively. The difference in the electron popula-
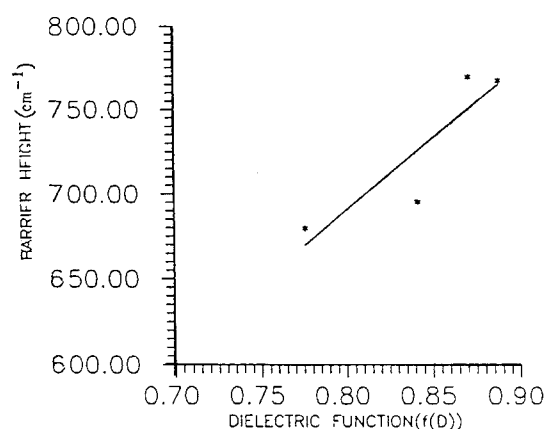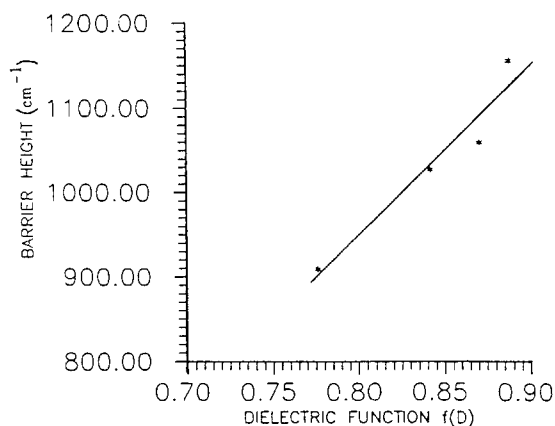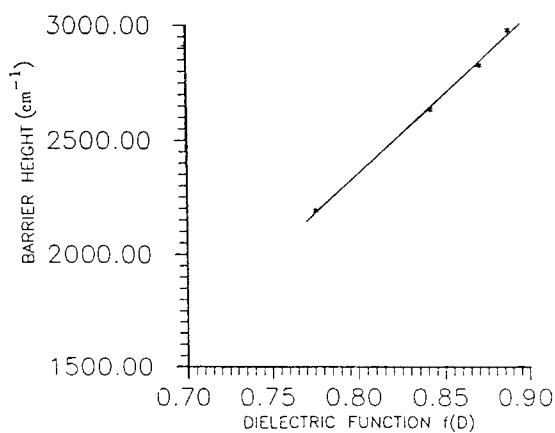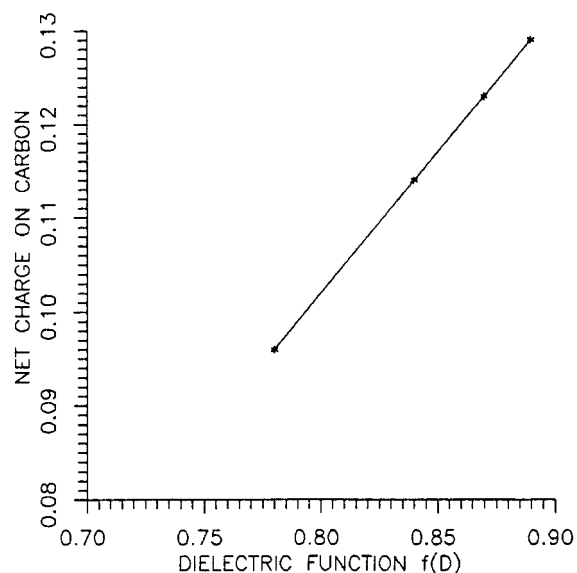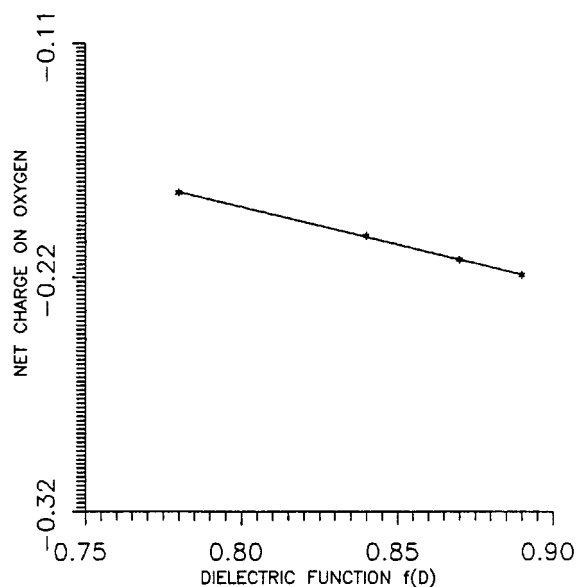
FIGURE 4. Inversion profile of fully relaxed H_2CO in solvents of dielectric (20–80) in $^3\pi\pi^*$ state.

FIGURE 5. Correlation of equilibrium out-of-plane bending angle ϕ for the fully relaxed H_2CO with dielectric function $f(D)$ in (a) $^1n\pi^*$, (b) $^3n\pi^*$ state.

tion in the valence orbitals on the carbon atom (e.g., $\Delta 2S$ and $\Delta 2P_z$) caused by relaxation of H_2CO in the $^3n\pi^*$ state in different solvents are recorded in Table VII. It is clearly seen that bending increases t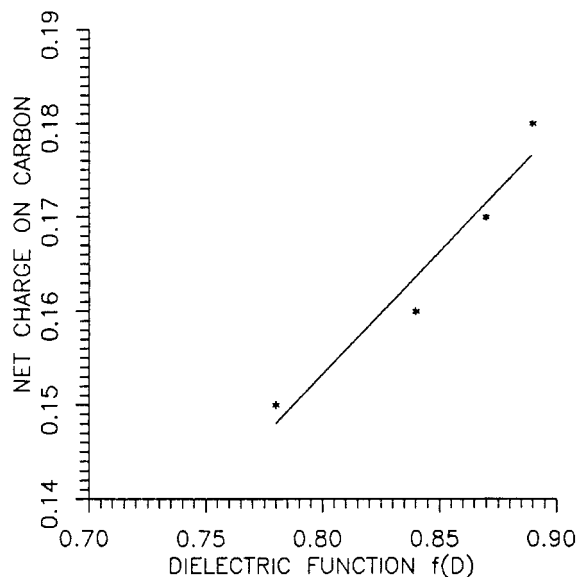he population of the $2S$ and $2P_x$ orbitals on the C atom and simultaneously depletes the electron density on the orbital of the C atom (the molecule in the XY plane — X lies along the C—O bond direction). The $2P_y$ population is, however, seen to be more or less immune to bending. The picture remains the same in any solvents irrespective of the magnitude of its polarity. It also transpires that the higher the polarity of the solvent the higher the value of the $|\Delta 2P_z|$. The in-
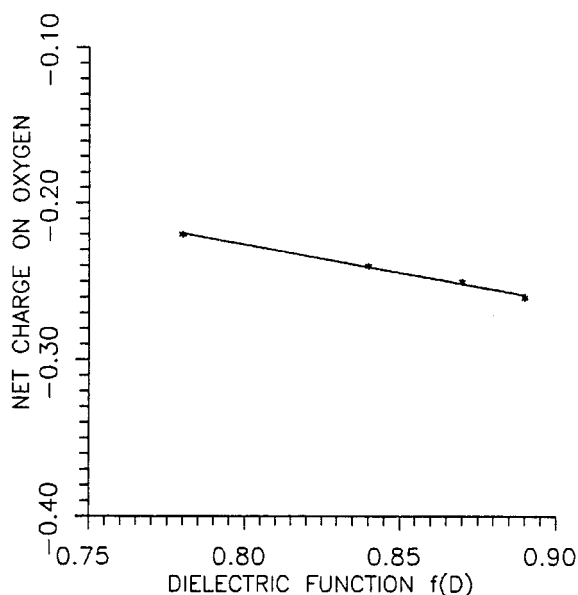
(a)

(b)

FIGURE 6. (a) Correlation of barrier height of H_2CO in the $^1n\pi^*$ with dielectric function $f(D)$ of the solvents in the fully relaxed inversion; (b) correlation of barrier height of H_2CO in the $^3n\pi^*$ with dielectric function $f(D)$ of the solvents in the fully relaxed inversion.

TABLE IV

Computed charge on carbon and oxygen atoms of formaldehyde in different solvents in the $^3n\pi^*$ state.

Dielectric constant (ε)	Equilibrium geometry charges on		Forced planar geometry charges on	
	C	O	C	O
1	-0.001	-0.075	-0.002	-0.073
20	0.096	-0.177	0.322	-0.164
40	0.114	-0.197	0.042	-0.183
60	0.123	-0.208	0.048	-0.199
80	0.129	-0.215	0.051	-0.199

One can therefore argue that macroscopic solvent polarization causes additional depletion of the electron density on the carbon $2P_z$ orbital over and above that caused by the relaxation brought in through out-of-plane bending and this increases the barrier to planar inversion in solvents of higher dielectric constants, when only nonspecific solvation effects are operative. Some macroscopic solvation-induced changes in the electron density observed for H_2CO in the $^1n\pi^*$ state follow the same pattern as already observed for the triplet state. It is clearly demonstrated that solvation causes further polarization of the electron density toward the oxygen atom. Table VIII shows (Δq), the difference between q(carbon) or q(oxygen) in $^{1,3}n\pi^*$ states, as function of solvent polarity. From the data, one can speculate that the additional polarization of the carbonyl charge distribution in the $^{1,3}n\pi^*$ is

FIGURE 7. Correlation of net charge on carbon with dielectric function $f(D)$ for the $^3n\pi^*$ state.

crease in $2S$ or $2P_y$ is, however, much smaller. The computed values of $|\Delta 2P_z|_{3n\pi^*}$ show linear correlation with the solvent dielectric function $f(D)$ (Fig. 8) and the computed barrier heights $(\Delta B)_{3n\pi^*}$ also correlate linearly with $|\Delta 2P_z|_{3n\pi^*}$ (Fig. 9).
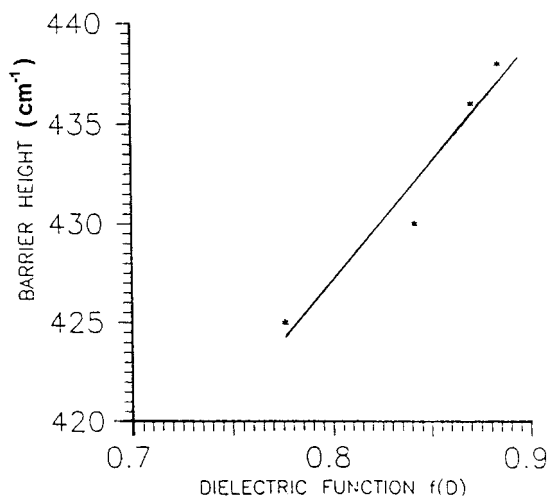
TABLE V
Electron densities on valence orbitals of the carbon atom in fully relaxed and forced planar H_2CO in the $^3n\pi^*$ state in different solvents.

Molecule in	Dielectric constant (ε)	2S	$2P_X$	$2P_Y$	$2P_Z$
Fully	1	1.170	0.843	0.933	0.950
relaxed	20	1.171	0.844	0.933	0.956
	40	1.175	0.843	0.934	0.933
	60	1.177	0.843	0.934	0.922
	80	1.178	0.842	0.934	0.916
Forced	1	1.110	0.770	0.933	1.150
planar	20	1.110	0.771	0.933	1.153
	40	1.113	0.766	0.935	1.144
	60	1.115	0.761	0.936	1.139
	80	1.115	0.759	0.937	1.137

TABLE VI
Electron densities on valence orbitals of carbon atom in fully relaxed and forced planar H_2CO in the $1n\pi^*$ state in different solvents.

Molecule in	Dielectric constant (ε)	2S	$2P_X$	$2P_Y$	$2P_Z$
Fully	1	1.14	0.84	0.92	1.03
relaxed	20	1.15	0.82	0.93	0.94
	40	1.15	0.82	0.93	0.93
	60	1.15	0.81	0.93	0.92
	80	1.15	0.81	0.93	0.92
Forced	1	1.10	0.82	0.92	1.11
planar	20	1.10	0.80	0.92	1.10
	40	1.10	0.79	0.93	1.09
	60	1.10	0.78	0.93	1.09
	80	1.10	0.78	0.93	1.09

TABLE VII
Differences of electron population in valence orbitals of carbon between fully relaxed and forced planar H_2CO in the $^3n\pi^*$ state.

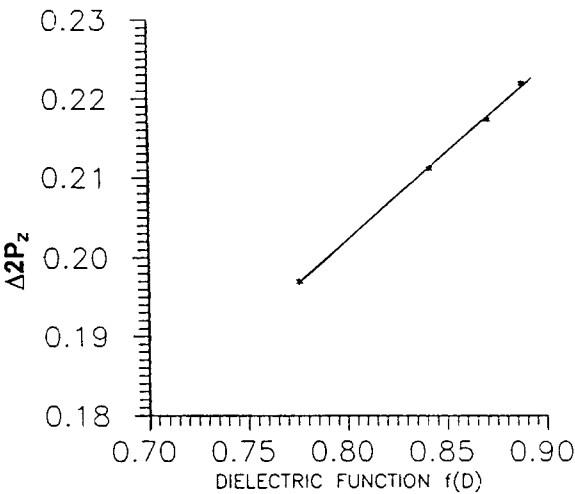| Dielectric constant (ε)	$\Delta 2S$	$\Delta 2P_X$	$\Delta 2P_Y$	$\Delta 2P_Z$
1	0.060	0.071	0.001	-0.196
20	0.060	0.072	0.001	-0.197
40	0.062	0.078	0.001	-0.211
60	0.062	0.082	0.002	-0.217
80	0.063	0.083	0.003	-0.222

FIGURE 8. Correlation of barrier height of unrelaxed H_2CO with dielectric function $f(D)$ at $^3n\pi^*$ state.

perhaps a consequence of Fermi correlation, which tends to thwart the $C \rightarrow O$ flow of electron density in the $^3n\pi^*$ state, thus opposing the consequences of solvent polarization on the $C=O$ charge distribution. The polarity-dependent inversion barrier in the $^1n\pi^*$ state has essentially the same origin as speculated for the triplet $^3n\pi^*$ state.
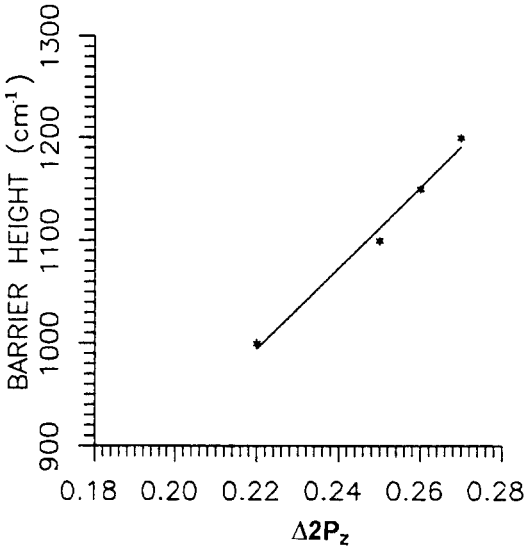

FIGURE 9. Correlation of computed values of $\Delta 2P_Z$ of fully relaxed H_2CO with dielectric function $f(D)$ in $^3n\pi^*$ state.

TABLE VIII
Computed charges on carbon and oxygen atoms of formaldehyde in different solvents in the $^1n\pi*$ state.

Dielectric constant (ε)	Equilibrium geometry charges on		Forced planar geometry charges on	
	C	O	C	O
1	0.06	−0.12	0.05	−0.11
20	0.15	−0.22	0.10	−0.21
40	0.16	−0.24	0.12	−0.23
60	0.17	−0.25	0.12	−0.24
80	0.18	−0.26	0.12	−0.24

TABLE X
Computed charges on carbon and oxygen atoms of H_2CO in different solvents in the $^3\pi\pi*$ state.

Dielectric constant (ε)	Equilibrium geometry charges on		Forced planar geometry charges on	
	C	O	C	O
1	0.164	−0.146	0.135	−0.140
20	0.306	−0.257	0.225	−0.246
40	0.335	−0.277	0.238	−0.265
60	0.347	−0.288	0.245	−0.274
80	0.355	−0.293	0.249	−0.274

We now turn to the behavior of the $^3\pi\pi*$ state of formaldehyde in different solvents. It is clear from the data summarized in Table IX that the polarization of electron density within the carbonyl group is much stronger compared to what has been observed in the $n\pi*$ states. The out-of-plane angle is also similarly affected by the solvent polarity. The electron population in different valence orbitals of the formaldehyde molecule in the forced planar and fully relaxed formaldehyde molecule in the $^3\pi\pi*$ state are recorded in Tables X and XI. Figure 10(a) and (b) reveals the linear correlation between the computed values of $\Delta 2P_z$ with the solvent polarity function and that of the inversion barrier heights with $2P_z$. A comparison with similar plots for the $n\pi*$ states suggests that solvent-assisted depletion of the $2P_z$ electron density on the C atom is much more pronounced in the $\pi*$ state. Although the discussion has been restricted to a prototypical molecule, the behavior noted for other tetraatomic carbonyls are virtually the same.

Conclusions

The macroscopic solvation purely controlled by the bulk solvent polarity may cause profound changes in the electronic distribution within the solute subsystem and thereby affect even intramolecular process like inversion. It leads one to speculate whether macroscopic solvation can influence specific solvation indirectly through solvation-induced changes in specific aspects of the

TABLE IX
Differences between the charge on carbon and oxygen atoms of fully relaxed H_2CO in the $3n\pi*$ state with those for the $^1n\pi*$ state.

Dielectric constant (ε)	$\Delta q_{3n\pi* - 1n\pi*}$ on	
	C	O
1	−0.0061	0.045
20	−0.054	0.043
40	−0.046	0.043
60	−0.047	0.043
80	−0.051	0.045

TABLE XI
Electron densities on valence orbitals of formaldehyde at forced planar and fully relaxed geometry in the $3\pi\pi*$ state in solvents of different dielectric constants.

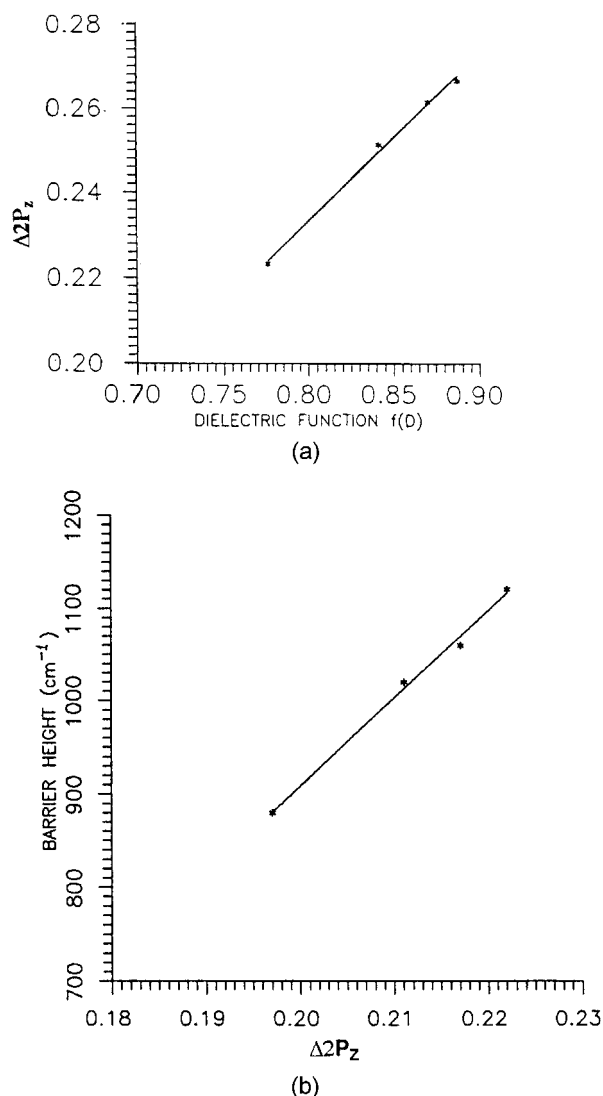|	Dielectric constant (ε)	2S	$2P_X$	$2P_Y$	$2P_Z$
Forced planar	1	1.11	0.73	0.91	1.00
	20	1.11	0.75	0.91	1.00
	40	1.11	0.73	0.91	1.00
	60	1.11	0.73	0.91	1.00
	80	1.11	0.73	0.91	1.00
Fully relaxed	1	1.17	0.83	0.91	0.79
	20	1.17	0.83	0.91	0.78
	40	1.18	0.83	0.91	0.75
	60	1.18	0.82	0.91	0.73
	80	1.18	0.82	0.91	0.73

FIGURE 10. (a) Correlation of net charge on carbon with dielectric function $f(D)$ in the fully relaxed $^1n\pi^*$ state; (b) correlation of net charge on oxygen with dielectric function $f(D)$ in the fully relaxed $^1n\pi^*$ state.

electronic structure of the solute to which the specific interaction is due. We hope to return to this topic in the near future.

References

1. E. S. Amis and J. F. Hinton, *Solvent Effects on Chemical Phenomena*, Vol. 1 (Academic Press, New York, 1973).
2. C. Reichart, Solvent Effects in Organic Chemistry (Verlag Chemie, Weinheiem, 1979).
3. P. Claverie, J. P. Dandy, J. Langlet, B. Pullman, D. Piazzola, and M. J. Huson, J. Phys. Chem. **82,** 405 (1978).
4. A. Pullman and A. M. Arunbruster, Chem. Phys. Lett. **36,** 558 (1975).
5. A. Pullman, in *The New World of Quantum Chemistry*, Proceedings of the Second International Congress of Quantum Chemistry, B. Pullman and R. G. Parr, Eds. (Reidel, Dordrecht, 1976), p. 149.
6. A. Pullman, in Quantum Theory of Chemical Relations, Vol. 3, R. Dandel, A. Pullman, L. Salem, and A. Veillard, Eds. (Reidel, Dordrecht, 1980), p. 1.
7. M. J. Huron and P. Claverie, Chem. Phys. Lett. **9,** 194 (1971).
8. J. O. Noell and K. Morokuma, Chem. Phys. Lett. **36,** 465 (1975).
9. L. Onsager, J. Am. Chem. Soc. **58,** 1486 (1936).
10. J. G. Kirkwood, J. Chem. Phys. **2,** 351 (1934).
11. D. L. Beveridge and G. W. Schnuelle, J. Chem. Phys. **79,** 2562 (1975).
12. J. Hylton, R. E. Christoftersen, and G. G. Hall, Chem. Phys. Lett. **24,** 501 (1974).
13. J. Rivail and D. Rineldi, J. Chem. Phys. **18,** 233 (1976); J. Comput. Chem. **6,** 155 (1982).
14. (a) R. Contreas and A. Aizman, Int. J. Quantum Chem. **27,** 293 (1983); (b) H. Hoshi, M. Sakurai, Y. Inove, and R. Cujo, J. Chem. Phys. **87,** 1107 (1987).
15. G. Klopman, Chem. Phys. Lett. **1,** 200 (1967).
16. H. A. Germer Jr., Theo. Chem. Acta **34,** 145 (1974).
17. O. Tapia and O. Goscinski, J. Molec. Phys. **29,** 1653 (1975).
18. R. Constanciel and O. Tapia, Theo. Chem. Acta **54,** 123 (1980).
19. M. M. Karelson, A. R. Katritzky, and M. C. Zerner, Int. J. Quantum Chem. Symp. **20,** 521 (1986).
20. E. Clementi, J. Chem. Phys. **54,** 2492 (1971).
21. J. Ladik and G. Biczo, J. Chem. Phys. **42,** 1658 (1965).
22. J. M. Andre, J. Chem. Phys. **50,** 1536 (1969).
23. O. Tapia, in *Quantum Theory of Chemical Reactions*, Vol. 3, (R. Dandel, A. Pullman, L. Salem, and A. Veillard, Eds. (Reidel, Dordrecht, 1980), p. 25.
24. M. D. Newton, J. Phys. Chem. **79,** 2795 (1975).
25. O. Tapia, in Molecular Interactions, Vol. 3, ch. 2, H. Ratajezak and W J. Orville, Eds. (Thomas New York, 1982).
26. S. Miertus and O. Kysel, J. Chem. Phys. **21,** 27 (1966).
27. W. Liptay, Z. Naturforche **A21,** 1605 (1966).
28. V. P. Senthilnathan and Surjit Singh, Spect. Chem. Acta **29,** 981 (1973).
29. J. M. Hichs, M. Vandersall, Z. Barbarogic, and K. B. Eisenthal, Chem. Phys. Lett. **116,** 18 (1985).
30. J. D. Simsons and S. G. Su, J. Phys. Chem. **94,** 3656 (1990).
31. A. Nag, T. Kundu, and K. Bhattacharyya, Chem. Phys. Lett. **160,** 257 (1989).
32. K. K. Das, D. Mukherjee, and S. P. Bhattacharyya, Int. J. Quantum Chem. **35,** 483 (1989).